

## **SIMULATION OF CANDU FUEL PIN THERMAL RESPONSE TO RIA POWER PULSE**

**T. Jafri<sup>1</sup>, T. Nitheanandan<sup>1</sup> and D. Caswell<sup>1</sup>**

<sup>1</sup> Atomic Energy of Canada Ltd., Chalk River, Ontario, Canada K0J 1J0

### **ABSTRACT**

An excursion in reactor power resulting from an increase in void reactivity is known as a power pulse. A large Reactivity Initiated Accident (RIA) database is available from experiments conducted with Light Water and Pressurized Water Reactor (LWR/PWR) fuels. This current study was undertaken to assess the applicability of this data for use in validating computer code predictions under CANDU reactor conditions. The study demonstrates that using short duration LWR/PWR power pulse data, with the same amount of specific energy deposition, is conservative with respect to fuel centre line temperature increases in comparison to using long duration CANDU power-pulse data.

### **1. INTRODUCTION**

A limited number of CANDU<sup>®1</sup> “power-pulse” tests were performed by the Industry in the Power Burst Test Facility (PBF) in Idaho Falls [1] during the early 1980’s. A large amount of data are also available [2] and [3] from a number of Reactivity Initiated Accident (RIA) experiments conducted mainly for PWR/LWR conditions. The enrichment of the fuel used in the PWR/LWR experiments is between 3.9 and 20.0%, which is different from CANDU fuel. The resulting power pulses in these experiments were narrow with pulse widths (i.e., time durations) ranging between 5 ms and 20 ms, whereas in CANDU fuels, the power-pulse width is of the order of 1-2 s.

The difference in the pulse width poses a general question: Could the datasets generated with short and high power pulse experiments be used for the validation of computer codes to predict the response of CANDU fuel which has power pulses two orders of magnitude longer?

This paper addresses the above question through the solution of the transient heat conduction equation. Calculations were performed using a time-dependent heat source, applied over a range of pulse widths that deposited the same cumulative energy. The simulations used a non-adiabatic and an adiabatic boundary condition. The resulting radial temperature profiles were examined. The computer code CATHENA MOD-3.5d/Rev 2 [4] was used for the simulations. The study was confined to the thermal aspects of power pulse only and the feedback from mechanical contributions was ignored.

During this study the following three input conditions were varied:

- Power-pulse shape – triangular and rectangular,
- Cumulative energy deposition – 343 and 490 kJ, and
- Radial power distribution – uniform and non-uniform.

---

<sup>1</sup>CANDU (CANada Deuterium Uranium) reactor is a registered trademark of Atomic Energy of Canada Limited (AECL).

## 2. POWER-PULSE TIME INTERVALS AND SPECIFIC ENERGY DEPOSITIONS FROM RIA EXPERIMENTS

The ranges of power-pulse time intervals and the resulting specific energy deposition reported in RIA experimental database are listed in the following Table 1. From the table it is apparent that CANDU fuel and the PWR/LWR fuels have almost similar specific energy deposition values even though the energy is deposited in a time period two orders of magnitude longer for CANDU fuel.

**Table 1**  
**Power-Pulse Characteristics**

Fuel Type	Power-Pulse Time Duration	Specific Energy Deposition, kJ/kg	Fuel Burnup Range, MWh/kgU
PWR/LWR	5 – 20 ms	250 – 1,007	0 – 1,200
CANDU	1 – 2 s	300 – 1,108	0 - 120

The general relationship between transient power input  $P(t)$ , cumulative energy deposition  $\Delta E$ , and power-pulse time interval  $\Delta t$ , is as follows:

$$\Delta E = \int_0^{\Delta t} P(t) dt \quad (1)$$

In the available RIA experimental data sets, it is this integrated or cumulative energy  $\Delta E$  that is reported at the time of fuel failure.

The one-dimensional transient heat conduction in the radial direction, with a time-dependent source term  $q_v(t)$ , is given as follows:

$$\frac{\partial}{\partial t} (\rho(T) C_p(T) T) + \frac{1}{r} \frac{\partial}{\partial r} (r k(T) \frac{\partial T}{\partial r}) = q_v(t) \quad (2)$$

where  $q_v = P(t) / (\text{Volume of the Fuel Pin})$ ,  $\rho$  is density,  $C_p$  is the specific heat,  $r$  is the radial distance,  $k$  is the thermal conductivity, and  $T$  is the temperature.

The common basis for the above equation is a unit volume, and the units of each term in the equation are  $\text{W/m}^3$ . Here,  $q_v(t)$  denotes the time-dependent heat source term, power input per unit volume of the fuel. During the simulations, the magnitude of  $q_v(t)$  is changed and the resulting radial temperature profile in  $\text{UO}_2$  part of the fuel pin is examined.

The following sections present three cases, and the corresponding parameter choices, used to examine the fuel thermal responses.

### 2.1 Case I: Adiabatic Boundary Condition (Uniform Initial Radial Temperature Distribution)

If a uniform radial temperature distribution,  $T(t=0)$ , is assumed for the fuel pin, the temperature difference between two consecutive points will be zero and the diffusion term, the 2<sup>nd</sup> term on the left hand side of Equation (2) drops out of the heat equation. The final fuel temperature, assuming temperature-independent physical properties, can be obtained analytically as follows:

$$T_{final} = T(0) + \frac{\int_0^{\Delta t} P(t) dt}{m C_p} \quad (3)$$

or,

$$T_{final} = T(0) + \frac{\Delta E}{mC_p} \quad (4)$$

This provides an estimate of the maximum temperature increase, in the absence of heat loss from the boundary and diffusion within the fuel pin.

Here, the symbols,  $m$  and  $C_p$ , represent mass and heat capacity of the fuel pin, respectively. For this uniform initial radial temperature and energy distribution case, all the radial nodes of the fuel pin will receive the same amount of heat energy and will undergo the same temperature increase. Because of the nature of the initial and boundary conditions, it is not relevant to the study proposed in this paper; however, it is provided here for completeness.

## 2.2 Case II: Adiabatic Boundary Condition (Non-Uniform Initial Radial Temperature Distribution)

The case of radial variation in the initial temperature distribution causes interaction of the power source term  $q_v(t)$  and thermal conductivity  $k(T)$  and hence would show the effect of heat diffusion on the transient response of the fuel pin.

For this case, the heat-transfer coefficient of the gap between the ceramic  $UO_2$  region and the fuel sheath is set to zero. The cumulative energy deposited is uniformly distributed in the radial regions (annuli) of  $UO_2$ . This case represents the adiabatic boundary condition as no heat flows from the surface boundary of the ceramic  $UO_2$ . Although the boundary condition appears to be unrealistic, the relevance will be established in Section 5.1.2.

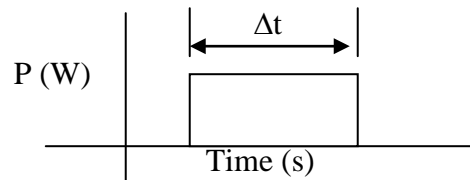
## 2.3 Case III: Non-Adiabatic Boundary Condition (Non-Uniform Initial Radial Temperature)

This model is designed to calculate the energy lost at the metal sheath surface during 5 ms, 1 s and 2 s power-pulse durations. A prescribed boundary condition at the outer surface of the metal sheath was applied with a heat-transfer coefficient of  $200 \text{ kW}/(\text{m}^2 \text{ K})$  between the outer sheath surface and a heat sink reservoir at  $320^\circ\text{C}$  (nominal coolant temperature and heat-transfer coefficients under typical normal operating conditions were assumed). The same non-uniform initial temperature distribution as in Case II was used. The heat-transfer coefficient for the gap between the fuel pellet and the metal sheath in this case was  $20 \text{ kW}/(\text{m}^2 \text{ K})$ .

For a non-uniform radial distribution of power, 10% excess fractional-power was deposited near the surface, to simulate the heat deposition from plutonium with a burnup of approximately  $60 \text{ MWh/kgU}$ . The excess fractional power input was deposited on the two outer annuli of the fuel pin where the cross-section of the pin was divided into 25 radial annulus regions. Each  $UO_2$  annular region has a thickness of  $0.243 \text{ mm}$ , which was based on typical CANDU pellet dimensions. The non-uniform distribution deposits 10% more power in annuli 24 and 25 over and above the base radial distribution for a given cumulative energy input, to simulate the near surface excess heat generation resulting from accumulated plutonium in the outer layers of the fuel pellets.

## 3. POWER-PULSE SHAPE

The simplest possible shape for a time dependent power pulse is a rectangular pulse. The power-pulse shape has a non-zero value during the time interval  $\Delta t$ . The time interval, 5 ms, 1 s or 2 s, was selected to be representative of the RIA data for CANDU and LWR/PWR reactors.



The amount of cumulative energy deposited for this shape is:

$$\Delta E = P(t) \Delta t \quad [5]$$

The implementation in CATHENA simply required specifying the magnitude of  $P(t)$  and time duration of the power pulse. CATHENA requires power input in Watts and calculates the volume of the fuel from the geometric information provided in the input file.

A representative magnitude for the power input,  $P(t)$  was obtained from the experimental data in Reference [1]. Variation in radial power deposition was applied by an additional record in the CATHENA generalized heat transfer package (GENHTP) model in the CATHENA input file.

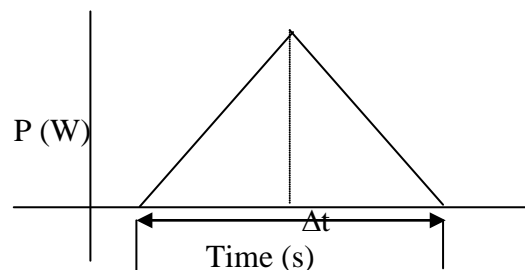
### 3.1 Triangular Power Pulse

For this power-pulse shape, the power is increased linearly and then decreased linearly in equal time intervals, as depicted in the sketch below. As mentioned earlier, the time interval  $\Delta t$  is the time duration during which the power pulse has a non-zero value. To estimate the cumulative energy in the triangular power pulse, the time interval is further divided into two equal sub-intervals, with increasing and decreasing input power ramp functions.

Mathematically,  $P(t) = a + b * t$ . Here  $a$ , and  $b$  are constants. These constants can be adjusted to obtain the desired cumulative energy input.

The cumulative energy deposition is again obtained by the integration.

$$\Delta E = \int (a + b * t) dt \quad [6]$$



Power  $P(t)$ , now has an explicit time dependence. The constants  $a$ ,  $b$  determine the rate of energy input and the desired cumulative energy to be deposited,  $\Delta E$ , over the time interval of interest.

For rectangular and triangular power-pulse shapes, if the time interval of energy deposition is increased, then there is a corresponding power decrease to keep the area under the curve, i.e., the cumulative energy deposition, constant. Figure 1 shows the power versus time graph for the 1 s time interval with rectangular and triangular power pulses. Each of these pulse shapes deposits 343 kJ of energy in 1 s.

## 4. CATHENA SIMULATIONS

The CANDU reactor thermalhydraulic safety analysis code, CATHENA was used to model the fuel response. The input file was designed to model adiabatic conditions and later modified for

non-adiabatic fuel pin response. For Case II fuel was modelled as one radial region with 26 radial nodes whereas for Case III fuel-sheath gap and metal sheath were also modelled with a total of 29 radial nodes. Node 1 denotes fuel centre line and node 26 denotes fuel surface.

## **5. RESULTS AND DISCUSSION**

The following section represents the fuel pin thermal response results for Case II and Case III parameter choices. The Case I parameter choice is not discussed in this section as it provided a flat temperature profile.

### **5.1 Case II: Simulations with Adiabatic Boundary Condition**

The simulation results for adiabatic boundary conditions are plotted in Figure 2 through Figure 4 and discussed in the following section.

#### **5.1.1 Rectangular Pulse with 343 kJ Cumulative Energy Input**

Figure 2 shows a comparison of the nodal temperature distribution for 343 kJ of cumulative energy input obtained with 5 ms and 1 s-long rectangular power pulses. The temperatures shown in the figure were obtained at the end of the simulation period (i.e., either 5 ms or 1 s depending on the duration of the pulse width). The initial temperature supplied to the model is also shown in the figure for comparison. For this simulation, the fuel pin was modelled under adiabatic conditions. The only mode of heat transfer available was conduction inside the fuel pin and therefore the fuel reaches an elevated temperature shown in the figure. The CANDU fuel pin temperatures with a 1 s-long pulse are lower than those using a 5 ms duration PWR/LWR power pulse up until the 20<sup>th</sup> node. The CANDU fuel temperature becomes higher for the 1 s-long pulse between the 20<sup>th</sup> and 26<sup>th</sup> nodes compared to the 5 ms-long pulse. This is indicative of the fact that during a 1 s-wide pulse, there is more time for the radial annulus near the surface to diffuse the heat towards the boundary compared to the 5 ms-wide pulse. Because of the radial diffusion of heat from the annulus sectors near the centre of the pellet in addition to the heat deposited by the applied power, the temperature in the 20<sup>th</sup> to 26<sup>th</sup> nodes are higher. Figure 2 quantitatively confirms that, for the same specific energy deposition, CANDU fuel maximum temperature and the thermal gradient is lower and therefore responds more benignly during a power pulse than PWR/LWR fuel.

Since fuel is a ceramic with low thermal conductivity, the temperature fields do not become uniform over the simulation time.

#### **5.1.2 Comparison of Rectangular and Triangular Pulse Shape with 343 kJ Cumulative Energy Input for Uniform and Non-Uniform Energy Distribution**

Figure 3 shows the radial temperatures distribution for a fixed 343 kJ cumulative energy input using 1 s long triangular and rectangular power pulses. The radial temperature distributions are identical for the rectangular and triangular power pulses with a fixed cumulative energy input. This result is consistent with our expectations since the cumulative energy deposition is same for both types of power pulses. Based on the comparison made in Figure 3, it can be concluded that the radial temperatures distribution is independent of the power pulse shape when the cumulative energy deposited into the fuel is equal under an adiabatic boundary condition.

Figure 4 shows the results at the end of the simulation period for non-uniform cumulative energy distribution (Case II, Section 2.3) in annuli 24 and 25 and with adiabatic boundary conditions. The distribution of the cumulative energy comparison shown in Figure 4 indicates that the non-uniform

radial power distribution of the cumulative energy in the fuel leads to a slightly higher fuel temperature in nodes 1 to 19 compared to uniform radial power distribution of cumulative energy deposition.

## 5.2 Case III: Simulation with Non-Adiabatic Boundary Conditions

The simulation with non-adiabatic boundary conditions was performed using the same initial temperature distribution as for the adiabatic boundary conditions.

The results are plotted in Figure 5, which presents the radial temperature distributions for 5 ms, 1 s, and 2 s power pulse widths. Since nodes at region boundaries are shared, there are a total of 29 nodes for fuel, gap and sheath together. The corresponding temperatures at these nodes, at the end of the power pulse, are plotted in this figure. The simulations indicate that the 5 ms-wide power pulse results in higher fuel temperatures than the 1 s and 2 s-wide power pulses. The solid vertical line in the figure represents the location of the fuel pellet boundary. The 5 ms-wide power pulse indicates a jump in the temperature at the boundary. The local peak observed in Figure 5 with the 5 ms power pulse is thus attributed to the dynamics of heat transfer from these two radial regions and the metal sheath surface. The temperature distribution smoothes out for 1 s and 2 s power pulse durations.

## 6. ENERGY LOSS CALCULATION

The integration of surface heat flux versus time curve gives the cumulative energy lost during the transient. The results are summarized in Table 2.

**Table 2**  
**Energy Lost from Outside Sheath Surface**  
**( $h = 200 \text{ kW/m}^2$ , Heat Sink Temperature =  $320^\circ\text{C}$ )**

	Power-Pulse Shape	Power-Pulse Width	Power Input, W	Cumulative Energy Input, kJ	Energy Lost, kJ	Comment
1	Rectangular	5 ms	6.86E07	343 kJ, (598 kJ/kg)	0.24 (0.07%)	Negligible Energy Loss (Adiabatic)
2	Rectangular	1 s	3.43E05	343 kJ	72.0 (21.00%)	
3	Rectangular	2 s	1.72E05	343 kJ	113.1 (32.98%)	
4	Rectangular	5 ms	9.80E07	490 kJ, (855 kJ/kg)	2.46 (0.50%)	Adiabatic
5	Rectangular	1 s	4.90E05	490 kJ	145.77 (29.75%)	
6	Rectangular	2 s	2.45E05	490 kJ	169.40 (34.57%)	

## 6.1 Discussion

Two sets of energy loss calculations are presented in Table 2. Entries 1 through 3 are for cumulative energy deposition of 343 kJ and entries 4 through 6 are for cumulative energy deposition of 490 kJ. It can be seen from Table 2 that for the 5 ms power-pulse width, there is negligible amount of energy lost, hence a power pulse with a time duration of the order of a few milliseconds can be treated as adiabatic.

It is seen from entries 2 and 3 that during the broad CANDU power pulse durations of 1–2 s, fuel would dissipate 21% and 33% of the cumulative energy input (343 kJ), respectively. This is because of the additional time available for heat transfer between the sheath surface and the coolant, when compared to a 5 ms-long power pulse. Similar trends are also seen for higher cumulative energy deposition of 490 kJ, as shown in entries 4 to 6.

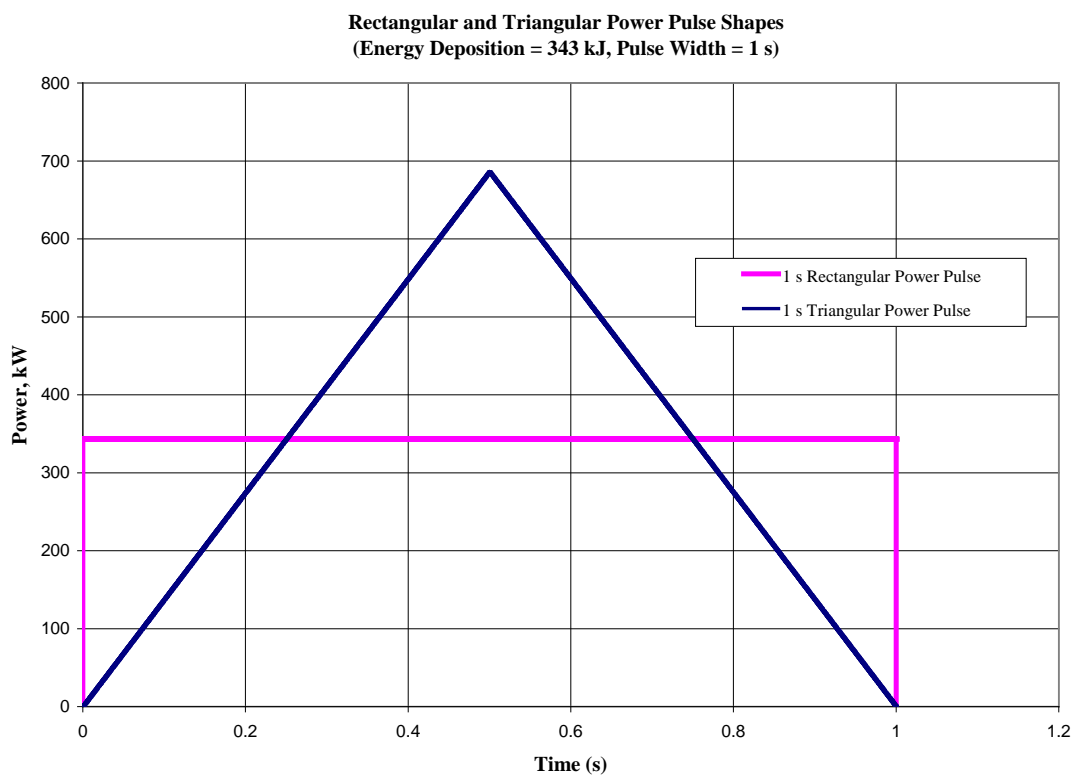


**Figure 1: Rectangular and Triangular Power-Pulse Shapes That Generate Same Amount of Cumulative Energy**

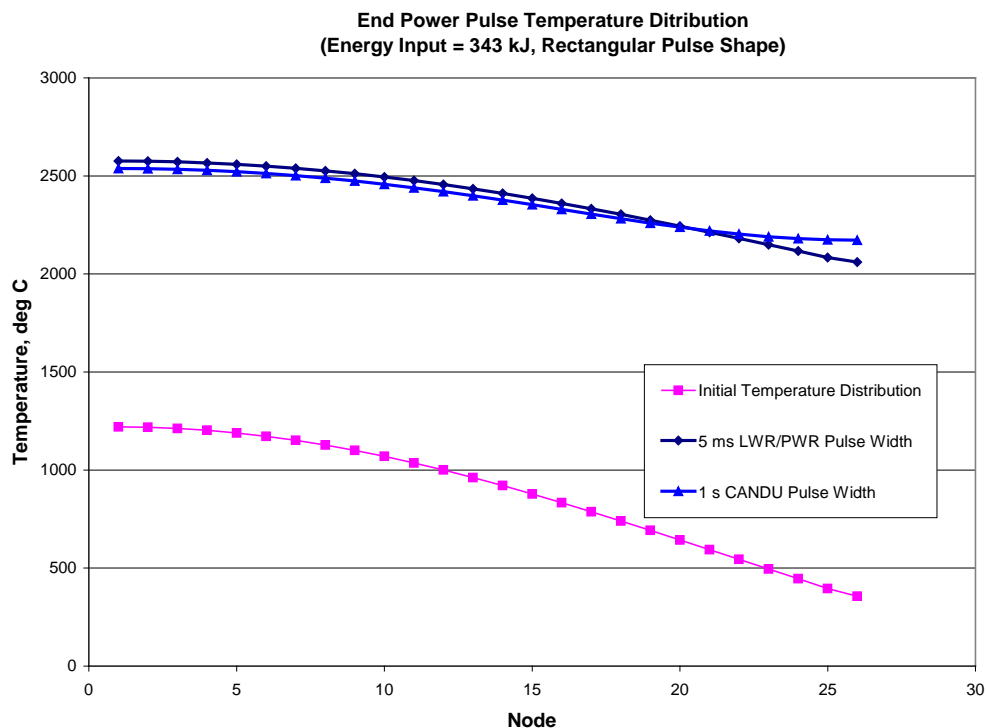


**Figure 2: Adiabatic Thermal Response for 343 kJ of Uniformly Distributed Cumulative Energy Input**

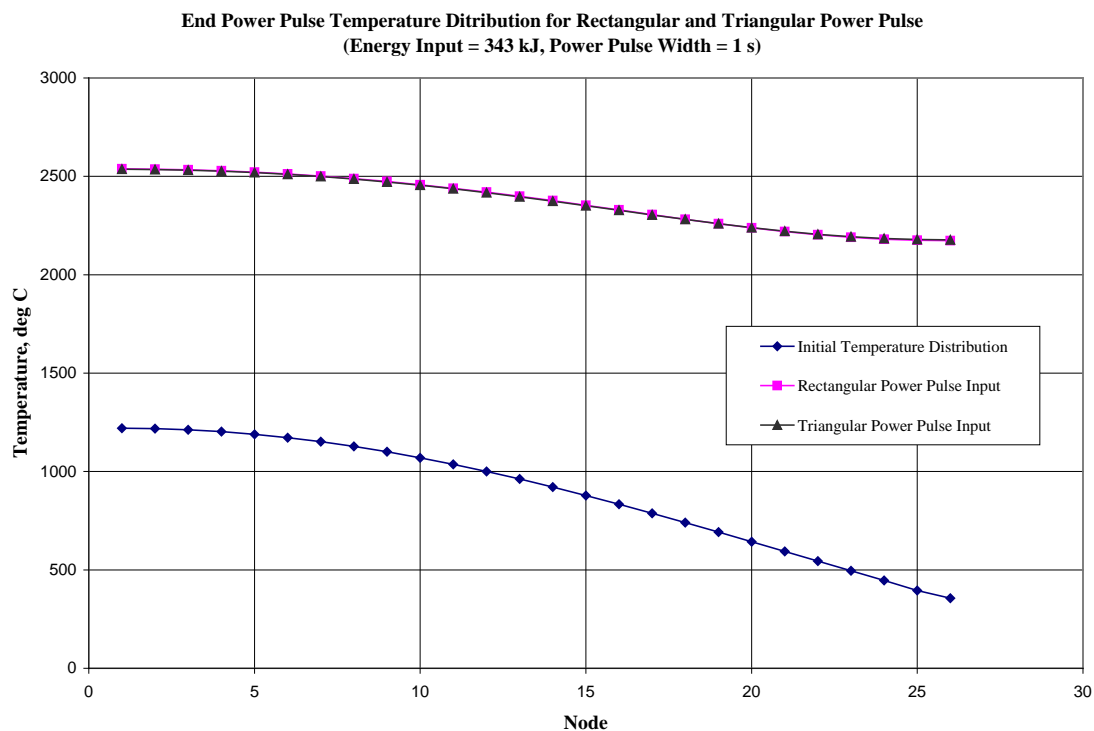


**Figure 3: Adiabatic Thermal Response for Triangular and Rectangular Power-Pulse Shape for 343 kJ of Uniformly Distributed Cumulative Energy Input**



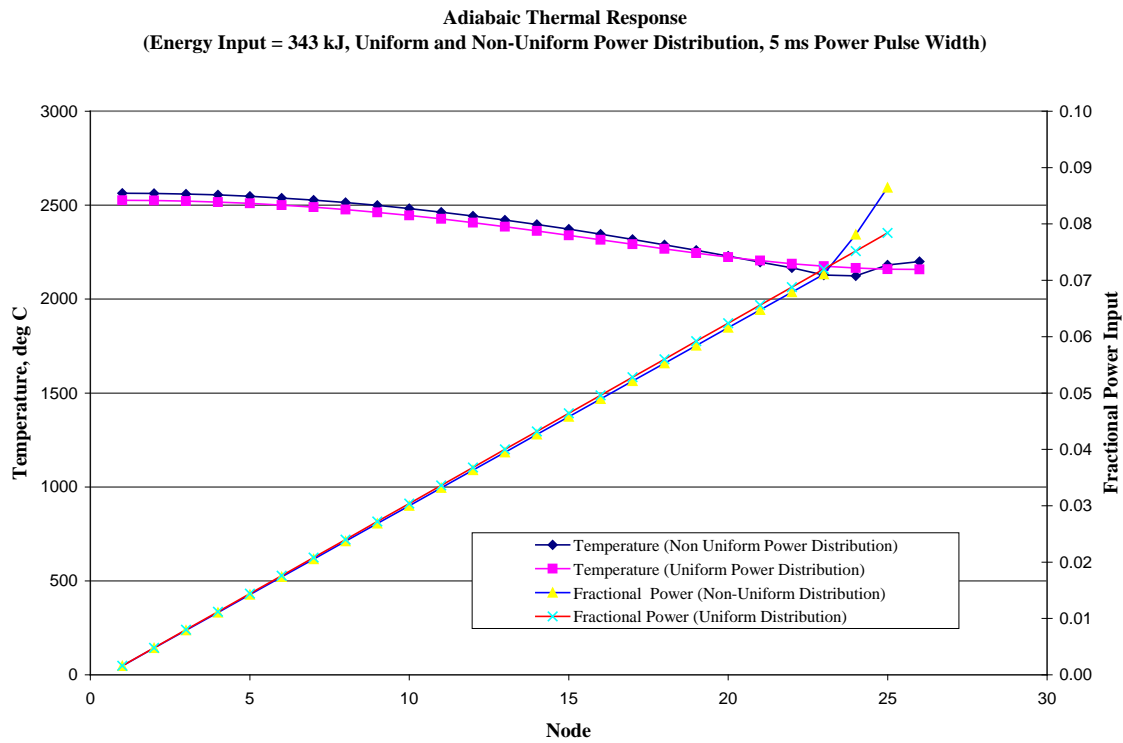


**Figure 4: Thermal Response for Non-Uniform and Uniform Cumulative Energy Distribution with Adiabatic Boundary Condition**

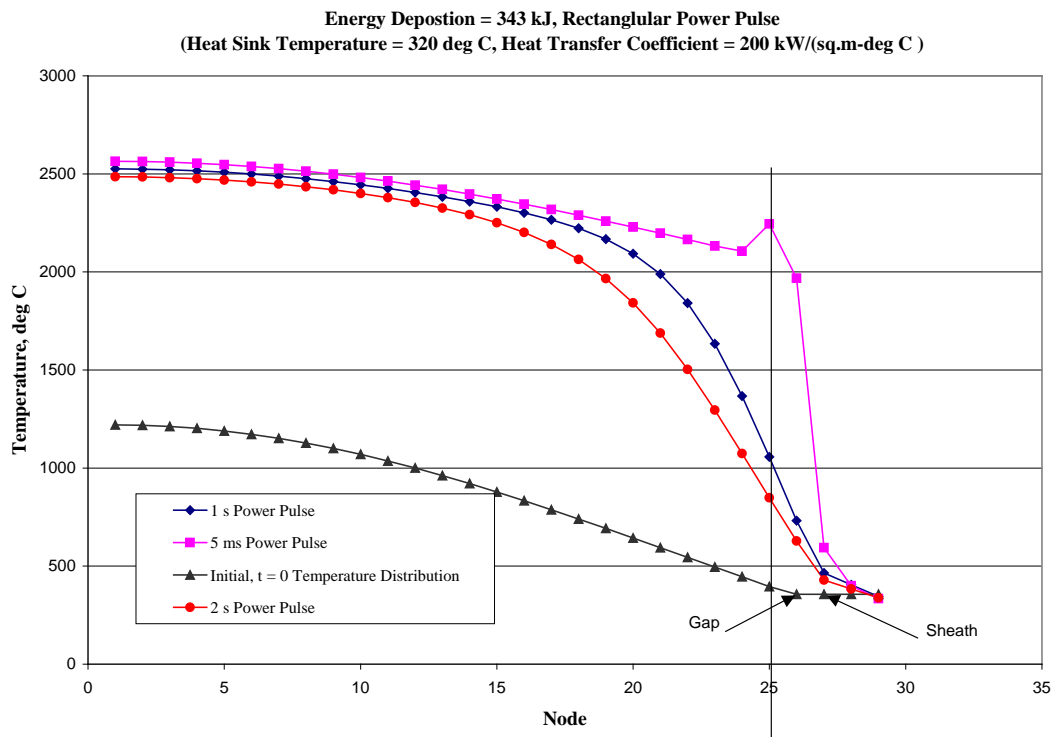


**Figure 5: Thermal Response for Non-Uniform Cumulative Energy Distribution with Non-Adiabatic Boundary Condition**

## 7. CONCLUSION

The study found that for adiabatic boundary conditions, the radial temperature distribution was independent of the power pulse shape, when the deposited cumulative energy is equal.

For non-adiabatic boundary conditions, the calculated fuel temperatures were higher for 5 ms-wide power pulses compared to 1 s and 2 s-wide power pulses. There was negligible amount of heat loss from the sheath for 5 ms-wide power pulses, and therefore the boundary conditions for short duration (i.e., ~5 ms) power pulses can be treated as adiabatic. In comparison, the longer duration power pulses had significant heat loss at the sheath boundary. Because of the heat loss at the sheath boundary, the longer power pulse experienced by CANDU fuel is more benign in terms of fuel centreline temperatures than that experienced by LWR/PWR fuel. It can, therefore, be concluded from these comparisons that using short duration LWR/PWR power-pulse data to validate fuel behaviour codes such as ELOCA, with same specific energy deposition, is conservative with respect to fuel centreline temperatures than CANDU power pulse experiments.

This analysis is a preliminary qualitative study intended to test the feasibility of the concept using very simplified boundary and initial conditions. A more detailed study may include the integrated effects of variable gap conductance, burn-up, realistic radial energy distribution, and the thermo-mechanical feedback.

## 8. ACKNOWLEDGEMENT

The work reported in this paper was funded by the COG R&D Safety and Licensing Program, under the joint participation of AECL, HQ, NBP, OPG, BP and SNN.

## 9. LIST OF ACRONYMS AND SYMBOLS

CANDU Canada Deuterium Uranium Reactor

CATHENA Canadian Algorithm for Thermalhydraulic Network Analysis

ELOCA Element Loss-of-Coolant Accident

LWR Light Water Reactor

PP Power Pulse

PWR Pressurized Water Reactor

RIA Reactivity Initiated Accident

Symbol	Description	Unit
a, b	Constants	
C <sub>p</sub>	Specific Heat	kJ/(kg K)
E	Internal Energy	kJ
k	Thermal conductivity	W/(m K)
m	Mass	kg
ms	milliseconds	
P	Power	W
q	Power input per unit volume	W/m <sup>3</sup>
r	Radius	m

s seconds

t Time s

T Temperature °C

### Subscripts

v Volume m<sup>3</sup>

### Greek

$\Delta$  Difference

$\rho$  Density kg/m<sup>3</sup>

## 10. REFERENCES

- [1] J. Adams and , R. K. McCardell, P. Kalis, R. McCormick and Z. R. Martinson, "PBF-CANDU Fuel Element Loss-Of-Coolant Accident Experiment Test Results Report", Report EGG-2384, Idaho National Engineering Laboratory, U.S. Department of Energy, 1985 May.
- [2] C. Vitanza, "A Review and Interpretation of RIA Experiments", Nuclear Engineering and Technology, Vol. 39, Iss. 5, pp. 591-602, 2007 October.
- [3] R. O. Meyer, "An Assessment of Fuel Damage in Postulated Reactivity Initiated Accidents", Nuclear Technology, Vol. 155, Iss. 3, pp. 293-311, 2006 September.
- [4] B. N. Hanna, "CATHENA: A thermalhydraulic code for CANDU analysis", Nuclear Engineering and Design, Vol. 180, Iss. 2, pp. 113-131, 1998.